

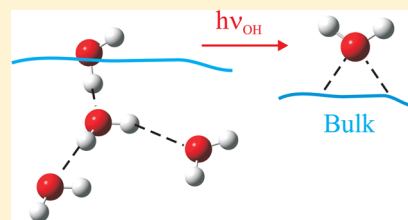
# IR Selective Irradiations of Amorphous Solid Water Dangling Modes: Irradiation vs Annealing Effects

J. A. Noble,<sup>†</sup> C. Martin,<sup>†</sup> H. J. Fraser,<sup>‡</sup> P. Roubin,<sup>†</sup> and S. Coussan<sup>\*,†</sup>

<sup>†</sup>Laboratoire Physique des Interactions Ioniques et Moléculaires, UMR 7345-CNRS, Aix-Marseille Université, Centre St-Jérôme, 13397 Marseille, Cedex 20 France

<sup>‡</sup>Astronomy Division, CEPsAR, Department of Physical Sciences, The Open University, Walton Hall, Milton Keynes MK7 6AA, U.K.

**ABSTRACT:** Amorphous solid water (ASW) is one of the most widely studied molecular systems. Ubiquitous in the interstellar medium (ISM) and potentially present in the upper layers of the Earth's atmosphere, ASW plays a major role in heterogeneous physical chemistry. Small molecules form or accrete at the ice surface, bonding to water molecules with an OH bond projecting from the surface, so-called "dangling bonds". These dangling OH are of crucial importance in the quest to identify and quantify surface reactions. Water ices in the ISM or Earth's atmosphere undergo constant processing by thermal and irradiation effects, which can significantly affect both the bulk and surface structures and therefore the catalytic properties of the surface. In this work we have studied thermal and irradiation processing of ASW and determine that there is a photochemical processing pathway of the ice surface which is clearly distinct from purely thermal effects. Selective IR irradiations of each of the surface water modes led to the observation of a "hole-burning" at the irradiation frequency, counterbalanced by the production of a new band, identified as a water monomer interacting with the surface. The thermal effects, meanwhile, led to a global decrease of all the dangling modes due to global reorganization of the water ice structure. It is thus obvious that, depending on the processing history of an ice, its catalytic properties will not be affected in the same way. The fact that we observe an IR selective irradiation effect illustrates that some fraction of the vibrational energy, rather than being relaxed through the H-bonded network of the bulk ice, is trapped at the surface; this energy induces a reorganization of the surface structure, forming new trapping sites, and thus generating new catalytic properties.



## I. INTRODUCTION

Amorphous solid water (ASW) is the most abundant water ice in the Universe, ubiquitous in the interstellar medium (ISM)<sup>1</sup> and postulated in the Earth's upper atmosphere.<sup>2–4</sup> Extensive studies of this material have been undertaken due to its interest in a wide range of scientific domains including chemistry, physics, astrophysics, and biology, and many in-depth books and review papers have been written.<sup>5–8</sup> The ASW structure is characterized by its hydrogen-bond network, its large surface area, and high porosity. In fact, its metastable amorphous structure can be used as a model of liquid water, and thus ASW is used to study supercooled liquids.<sup>9</sup> Because of its presence in key interstellar environments, such as molecular clouds<sup>10–13</sup> and comets,<sup>14</sup> ASW is believed to be intimately involved in the formation of so-called prebiotic molecules and thus in the origins of life.<sup>15</sup>

The ASW surface is of particular interest due to its catalytic role in chemical reactions. It has long been known that, in the ISM, molecules form and accrete on the surface of dust grains. In molecular clouds, these microscopic siliceous and carbonaceous particles become covered in a layer of ice, which is predominantly composed of H<sub>2</sub>O. Upon the surface of this ASW mantle, small molecules such as H<sub>2</sub>,<sup>16,17</sup> O<sub>2</sub>,<sup>18</sup> H<sub>2</sub>O, NH<sub>3</sub>,<sup>19</sup> CO<sub>2</sub>,<sup>20–22</sup> CO,<sup>23</sup> HCl,<sup>24</sup> and dicyanoacetylene<sup>25</sup> form or accrete from the gas phase. Once present on the ASW surface, these small molecules can undergo further radical,

thermal, and radiative processes, inducing reactions leading to more complex molecules, such as the hydrogenation of CO to form CH<sub>3</sub>OH.<sup>26</sup> Ultimately, it is believed that prebiotic molecules, precursors to amino acids, form on the ASW surface<sup>27</sup> due to its catalyzing effect. ASW in the form of either nanoparticles<sup>28,29</sup> or a film accreted on a grain will undergo processing events such as heating<sup>30</sup> and/or irradiation<sup>31</sup> in both the upper layers of the Earth's atmosphere or in the ISM; such processing dramatically affects both its bulk and surface structures.

ASW was first produced in the laboratory<sup>32</sup> in 1935 and has since been extensively characterized.<sup>5,8</sup> Its bulk structure is a four-coordinated tetrahedral arrangement, much like crystalline water ices. Molecules at the surface occupy one of four orientations: a four-coordinated molecule bound in a modified tetrahedron structure, known as s4; a tricoordinated molecule with one lone electron pair exposed at the surface, dO; a tricoordinated molecule with one OH dangling from the surface, dH; and a bicoordinated molecule with one lone pair and one OH dangling from the surface, dH. These orientations, or surface modes, exhibit vibrational frequencies at 3503, 3549, 3698, and 3720 cm<sup>−1</sup>, respectively, as outlined in Table 1.<sup>28,33,34</sup>

Received: July 11, 2014

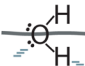
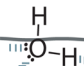
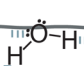
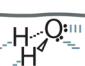
Revised: July 29, 2014

Published: July 30, 2014



Much work has already been done to characterize these surface modes, including their behavior upon heating<sup>28</sup> and upon adsorption of small molecules.<sup>35,36</sup>

**Table 1. Surface Modes of Water in ASW**

Notation	dH	dH	dO	s4
Coordination	2	3	3	4
Frequency /cm <sup>-1</sup>	3720	3698	3549	3503
Orientation				

We recently published a letter<sup>37</sup> in which we described the effect of IR selective irradiations upon the surface modes of ASW. While the desorption of water molecules from a polycrystalline ice, provoked by irradiation of the bulk water vibrational mode centered at  $\sim 3300$  cm<sup>-1</sup>, was described by Focsa et al.,<sup>38</sup> ours was the first study of the IR selective irradiation of an ASW surface. Upon irradiation of each of the four identified surface modes, a “hole-burning” event was observed at the irradiation frequency, indicating the loss of oscillators at this frequency; additionally, a new band at 3725 cm<sup>-1</sup> was observed. This new band was attributed to a H<sub>2</sub>O monomer on the ASW ice, stabilized by the presence of nitrogen accreted from the gas phase. In this paper, we extend our earlier, preliminary work to consider three different irradiation scenarios as well as a detailed comparison with annealing effects. The aim of our study is to more extensively investigate the effects of selective irradiation upon a water ice sample and to discriminate between thermal and irradiation effects. Although we are able to suggest a postirradiation surface structure, there remain some unanswered questions, such as what mechanism is involved in this surface reorientation, or “isomerisation”? We discuss relaxation pathways of the energy through the bulk water ice and the surface layers, providing possible photochemical scenarios for the surface pathway that include water monomer desorption and reorientation, or “flipping”, of water molecules. Comparison of our irradiation experiments with thermal experiments allows us to discriminate between these different physicochemical processes, confirming our definition of the postirradiation ASW surface structure.

## II. EXPERIMENTAL SETUP

ASW samples were prepared as follows: deionized water was subjected to multiple freeze–pump–thaw cycles under vacuum to remove dissolved gases. Mixtures of purified H<sub>2</sub>O and helium (Air Liquide,  $\geq 99.9999\%$ ) gas were prepared in a ramp with a base pressure of  $10^{-4}$  mbar at a ratio of H<sub>2</sub>O–He = 1:25. Ices were produced by depositing the gas mixture directly onto a gold-plated copper surface held at 50 K (to avoid trapping of the vector gas or nitrogen) then cooled to 3.7 K (the cooling typically takes around 5 min due to the high power of the cryogenerator (PT-405 Cryomech, 0.5 W at 4 K)). IR spectra were recorded in reflection mode using a Bruker 66/S FTIR spectrometer equipped with a KBr/Ge beamsplitter and a MCT detector (4000–800 cm<sup>-1</sup>, 0.12 cm<sup>-1</sup> resolution, 500 scans).

The dangling OH bond region of the IR spectrum of a typical ASW sample is presented in Figure 1, spectrum a. The two dH bands, centered at 3720 and 3698 cm<sup>-1</sup> are visible in the spectrum. A mass spectrometer (Hiden HAL 301) is attached to the vacuum chamber. The base pressure in the

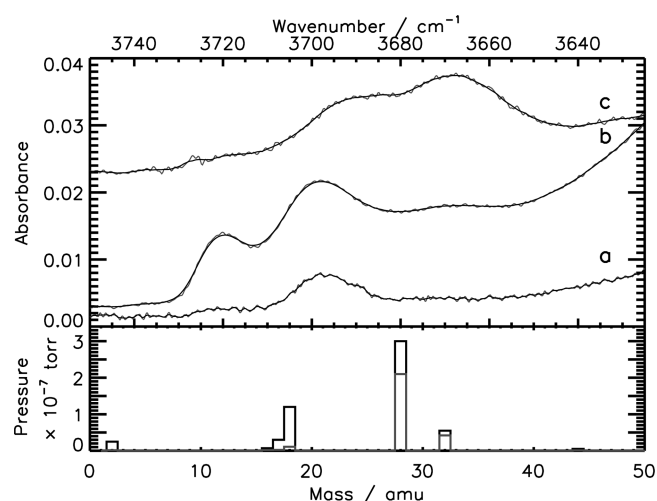


**Figure 1.** Deposition conditions in the experimental setup. Upper panel: Spectra (at 3.7 K) of the ices (a) 1:25 H<sub>2</sub>O–He deposited at 50 K, (b) 1:25 H<sub>2</sub>O–He deposited at 3.7 K, and (c) 1:10:250 N<sub>2</sub>–H<sub>2</sub>O–He deposited at 10 K. Lower panel: Mass spectra of the residual vacuum in the high vacuum chamber at 300 K (black) and 5 K (gray).

vacuum chamber is  $10^{-7}$ – $10^{-6}$  mbar at room temperature, decreasing to  $10^{-8}$ – $10^{-7}$  mbar at 3.7 K due to cryopumping of molecules. In the lower panel of Figure 1, we present mass spectra of the residual vacuum at 300 K (black) and after cooling to 5 K (gray). It is clear that nitrogen ( $m/z$  28) is the dominant pollutant at both room temperature and after cooling of the surface but that both N<sub>2</sub> and H<sub>2</sub>O ( $m/z$  18,17) abundances decrease significantly upon cooling.

The effect of N<sub>2</sub> on the deposited H<sub>2</sub>O samples is illustrated in the upper panel of Figure 1. Spectrum a is a typical ASW sample deposited at 50 K; spectrum b is the same H<sub>2</sub>O–He mixture deposited at 3.7 K; and spectrum c is a 1:10:250 N<sub>2</sub>–H<sub>2</sub>O–He mixture deposited at 10 K. It is clear that in spectra b and c there is a peak centered at 3667 cm<sup>-1</sup>, which we attribute to the presence of nitrogen.<sup>39</sup> The two dangling bond peaks are more pronounced in the nitrogen polluted spectrum b. This is due to a combination of factors: deposition at lower temperature enhances the formation of a porous ice<sup>40</sup> and nitrogen magnifies the dangling bond peaks.<sup>41</sup> Thus, deposition at 50 K produces ices with less prominent dangling bond features but is necessary in order to ensure that the original deposited ices are not polluted by nitrogen.

After deposition, ices were subjected to one of two types of experiment: global annealing of the whole sample or selective irradiation of the surface modes. Irradiations were performed using a tunable IR OPO Laserspec (1.5–4  $\mu$ m), pumped at 10 Hz by a pulsed Nd:YAG Quantel Brilliant B laser (1064 nm, pulse duration 6 ns). The average power is  $\approx 35$  mW in the  $\nu_{OH}$  domain, except in the range 3520–3500 cm<sup>-1</sup> where it is  $\approx 10$  mW, with a fwhm  $\geq 1.5$  cm<sup>-1</sup>, and each irradiation was performed for 1 h to achieve saturation of the effects.

In order to investigate the energy dissipation mechanisms involved in ASW, three types of irradiation experiments were carried out: the irradiation of a new ASW sample at a single frequency; suites of irradiations on a single ASW sample, carried out at each surface mode frequency in turn (from red to blue and vice versa); and back irradiation on bands formed during initial irradiation of surface modes.

### III. RESULTS AND DISCUSSION

**III.A. Annealing Experiments.** Many studies have been performed on the annealing of ASW, in particular with relation to its dangling OH bonds; it has been shown that heating an ASW sample reduces the intensity of the dH bands at 3720 and 3698  $\text{cm}^{-1}$  due to the compactification and crystallization of the ice.<sup>39,42</sup> We performed annealing experiments upon our deposited ASW in order to verify our deposition method. The results of these experiments are presented in Figure 2.

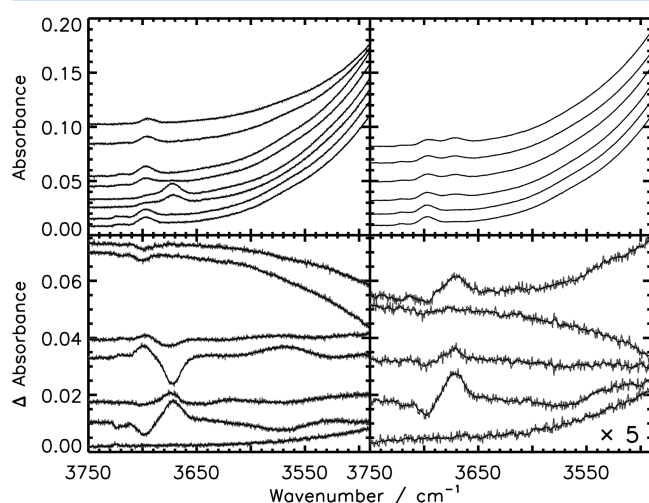


**Figure 2.** Annealing experiments on ASW samples. Left hand side: Simple heating from 3.7 to 100 K. Individual spectra (upper panel) were taken at (bottom to top) 3.7, 10, 20, 30, 40, 50, 75, and 100 K. The lower panel shows the difference spectra of (bottom to top) 10–3.7, 20–10, 30–20, 40–30, 50–40, 75–50, and 100–75 K. Right hand side: Cyclical heating and cooling of an ASW sample. The individual spectra (upper panel) were taken at (bottom to top) 4, 10, 15, 10, 4, and 15 K. The lower panel shows the difference spectra of (bottom to top) 10–4, 15–10, 10–15, 4–10, and 15–4 K.

The first annealing experiment, presented in the two left-hand panels of Figure 2, was a simple heating experiment. The upper panel shows the IR spectra in the range 3750–3450  $\text{cm}^{-1}$ , with the temperature increasing from 3.7 K (bottom spectrum) to 100 K (top spectrum), while the lower panel shows the difference spectrum for each temperature increase, again presented from bottom to top, lowest to highest. Considering the IR spectra in the top panel, it is clear that the position of the dangling bond peaks shifts redwards between 10 and 20 K (the second and third spectra, respectively) before returning to the original position between 30 and 40 K (the fourth and fifth spectra, respectively). By considering the difference spectra (lower panel), we can extract more details: between 10 and 20 K, decreases at 3719 and 3699  $\text{cm}^{-1}$  (and a larger, weaker signal centered at  $\sim 3570 \text{ cm}^{-1}$ ) are offset by an increase at 3672  $\text{cm}^{-1}$ ; this band continues to grow until 30 K, after which the changes are reversed between 30 and 50 K. At 75 and 100 K there is evidence of the decrease in intensity of the dH bands. The band at 3672  $\text{cm}^{-1}$  which appears between 10 and 20 K is characteristic of  $\text{N}_2$  adsorbed upon the dH bands<sup>36</sup> and, based upon its binding energy,  $\text{N}_2$  likely becomes mobile on the ASW surface at  $\sim 12$ –15 K and starts to desorb above  $\sim 20 \text{ K}$ .<sup>30</sup> These results suggest that, despite our deposition methodology,  $\text{N}_2$  is present at low levels on the gold-coated copper surface or in the deposited ice. On

the basis of the spectra in Figure 1, it is clear that if  $\text{N}_2$  is present in our ice, it is present as a trace pollutant, at a concentration significantly lower than 10%. Before deposition,  $\text{N}_2$  from the vacuum chamber freezes onto the coldfinger during cooling of the surface from room temperature to experimental temperatures of  $\sim 3.7 \text{ K}$ . The decrease of pressure in the vacuum chamber is on the order of 1 order of magnitude, thus in a chamber of  $\sim 26 \text{ L}$  corresponds to only  $\sim 10^{15}$  molecules. However, at a pressure of  $10^{-8} \text{ mbar}$ ,  $\text{N}_2$  molecules will adsorb on the cold surface at a rate of approximately 8 mL  $\text{h}^{-1}$  and therefore between the spectra measured at 3.7 and 20 K, up to 12 mL could potentially have accreted from the chamber. It is therefore unsurprising that, despite its very high surface area, a very low level of  $\text{N}_2$  pollution is observed in our ASW. As will be discussed in section III.B this is, in fact, advantageous in these experiments, as it allows us to identify the product of selective irradiation of the surface modes of ASW.

The second annealing experiment, presented in the two right-hand panels of Figure 2, included a thermal cycle where the ice was heated, cooled, and then reheated. As for the simple annealing experiment, the upper panel shows the IR spectra in the wavenumber range 3750–3450  $\text{cm}^{-1}$ , with ice temperatures of 3.7, 10, 15, 10, 4, and 15 K (bottom to top), while the lower panel shows the difference spectrum between each temperature change. It should be noted that the difference spectra have been multiplied by a factor of 5 to aid interpretation of the data. In this experiment, almost no difference is seen upon heating from 3.7 to 10 K. Upon heating to 15 K, decreases centered at 3700 and  $\sim 3570 \text{ cm}^{-1}$ , as well as an increase at 3671  $\text{cm}^{-1}$ , are observed. When the ice is then cooled to 10 K, a slight decrease at 3700 and slight increase at 3671  $\text{cm}^{-1}$  are observed, but this is likely due to changes in the ice while still at elevated temperatures (during cooling). At 4 K, no difference in the dangling modes is observed. However, upon reheating to 15 K, a decrease at 3700 and an increase at 3671  $\text{cm}^{-1}$  are again observed. We can draw two conclusions from these data: that the redistribution of the  $\text{N}_2$  in/on the ice is a dynamic process at 15 K which recommences after a thermal cycle, continuing as surface temperatures increase to approximately 30 K (see Figure 2 lower left-hand panel) and that the process is irreversible upon cooling, i.e., the  $\text{N}_2$  does not return to its original environment once it has migrated. It can therefore be inferred that adsorption on the dangling OH bonds represents a favorable energy configuration for the  $\text{N}_2$  molecules.<sup>43</sup>

These annealing experiments helped to characterize ice typical of that upon which irradiation experiments were carried out.

**III.B. Individual Irradiation Experiments.** Single frequency, postdeposition selective irradiations of each of the four ASW surface modes were performed. These data were previously discussed in Noble et al.<sup>37</sup> and are summarized in Figure 3. In the main panel of Figure 3 we present the difference spectra of a pure ASW sample irradiated at 3503 (s4, 1), 3549 (dO, 2), 3698 (dH, 3), and 3720  $\text{cm}^{-1}$  (dH, 4). Upon each irradiation we observe a very similar result, namely, that a hole appears at (or up to 3  $\text{cm}^{-1}$  red-shifted from) the frequency of irradiation and that a new peak appears at 3725  $\text{cm}^{-1}$ . The “hole-burning” effect results from the decrease in OH oscillators at the irradiated frequency, due to the reorientation, or “flipping” of irradiated  $\text{H}_2\text{O}$  molecules, while the newly formed band at 3725  $\text{cm}^{-1}$  is due to the formation of a new  $\text{H}_2\text{O}$  surface mode.



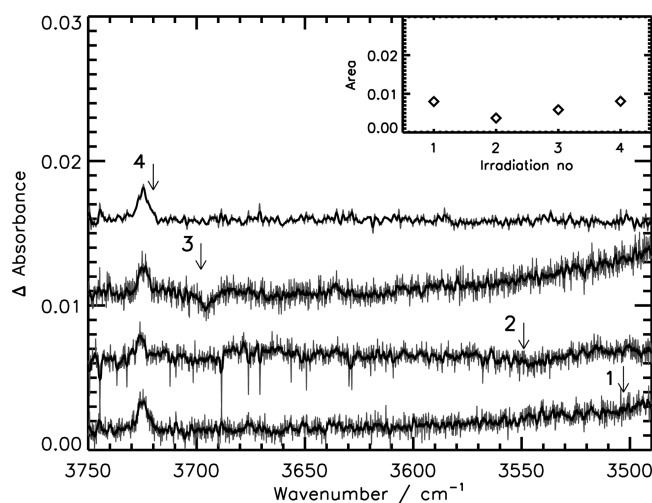


**Figure 3.** Individual irradiations of ASW samples at the surface mode frequencies. Main panel: Spectra in gray are difference spectra taken after irradiation at (1) 3503  $\text{cm}^{-1}$ , (2) 3549  $\text{cm}^{-1}$ , (3) 3698  $\text{cm}^{-1}$ , and (4) 3720  $\text{cm}^{-1}$ . In this and all subsequent figures, the arrows represent the frequencies of irradiation specific to each difference spectrum and overplotted in black are the difference spectra smoothed over 20 data points. Inset: The area under the band at 3725  $\text{cm}^{-1}$  is plotted for each difference spectrum.

In Figure 3 the “hole-burning” effects are most evident in spectra 3 and 2. In spectrum 4, the “hole-burning” is masked by the growth of the band at 3725  $\text{cm}^{-1}$ , while in spectrum 1, the irradiated band is significantly wider than the other surface modes, due to the large number of potential orientations in the s4 mode.<sup>34</sup> A second, smaller peak is seen in spectrum 3 at 3638  $\text{cm}^{-1}$ . The new  $\text{H}_2\text{O}$  surface mode responsible for the band at 3725  $\text{cm}^{-1}$  (and the small band at 3638  $\text{cm}^{-1}$  in spectrum 3) was identified as an  $\text{H}_2\text{O}$  monomer on the ice surface complexed by  $\text{N}_2$  molecules. Full details of the assignment are given in Noble et al.<sup>37</sup> In summary, the newly formed monomer species was identified based upon a series of background deposition experiments of water, nitrogen, and mixtures of  $\text{H}_2\text{O}-\text{N}_2$ . The background deposition of either pure  $\text{H}_2\text{O}$  or pure  $\text{N}_2$  onto an ASW sample did not provoke the growth of new bands in the IR spectrum. Deposition of  $\text{H}_2\text{O}$  followed by  $\text{N}_2$  provoked the appearance of a band at 3725  $\text{cm}^{-1}$ , while deposition of a  $\text{H}_2\text{O}-\text{N}_2$  mixture (1:10) resulted in the growth of a pair of bands at 3725 and 3638  $\text{cm}^{-1}$ .<sup>44</sup> We are therefore confident in our assignment of the 3725  $\text{cm}^{-1}$  band (occasionally accompanied by a weak signal at 3638  $\text{cm}^{-1}$ ) to  $\text{H}_2\text{O}$  complexed by  $\text{N}_2$ .

As was explained in section II,  $\text{N}_2$  is the major contaminant in the vacuum chamber; as such, there is a constant but very low level deposition of  $\text{N}_2$  molecules onto the ice surface during experiments. Because of the residual presence of  $\text{H}_2\text{O}$  in the chamber after deposition of the ASW sample, some  $\text{H}_2\text{O}$  also deposits onto the surface, and thus a  $\text{N}_2-\text{H}_2\text{O}$  matrix develops over the course of several hours. This adds a small background contribution to the band at 3725  $\text{cm}^{-1}$  but is minimal compared to the effect of irradiation over the course of 1 h. Additionally, the complexification of the OH oscillators by  $\text{N}_2$  also induces an amplification<sup>41</sup> of the signals at 3725 and 3638  $\text{cm}^{-1}$  and thus magnifies the newly formed bands, which is particularly important for observation of the weak signal at 3638  $\text{cm}^{-1}$ . The inset in Figure 3 displays the area under the newly formed band at 3725  $\text{cm}^{-1}$  due to irradiation. The values

have been corrected for the low level background deposition of  $\text{N}_2-\text{H}_2\text{O}$  on the surface by subtraction of the area under the 3725  $\text{cm}^{-1}$  peak after 1 h without irradiation. The number of molecules contributing to the 3725  $\text{cm}^{-1}$  band differs between the different irradiations, suggesting that the formation of the 3725  $\text{cm}^{-1}$  band is not a single, simple process but rather related to the individual oscillator classes excited by irradiation. Indeed, depending on the excited oscillators, the pathway by which the vibrational relaxation takes place could be completely different, leading to different results for different surface modes. A molecule in a dO or s4 configuration is not coupled with the H-bond network in the same way as a molecule in a dH configuration. As a result, in the case of a selective irradiation, the ratio of isomerized/nonisomerized surface molecules is not the same for all surface modes.

There are two important points to note regarding the individual postdeposition irradiation experiments. First, both the decreasing (particularly at 3698  $\text{cm}^{-1}$ ) and increasing (3725  $\text{cm}^{-1}$ ) bands are relatively narrow (fwhm  $\approx 5 \text{ cm}^{-1}$ ), implying that, despite the fact that ASW is an amorphous, disordered solid<sup>7</sup> with inhomogeneously broadened absorption bands, only certain classes of oscillators are able to (or are provoked to) isomerize upon selective irradiation of a given absorption band. The “hole-burning” observed upon irradiation of the dO band (3549  $\text{cm}^{-1}$ ) is significantly wider, implying either that the range of oscillators excited by this irradiation was also wider or that the oscillators are more coupled in this surface mode. The fact that we see a clear decrease of a limited class of oscillators implies that the induced reorientations of  $\text{H}_2\text{O}$  molecules do not occur randomly but rather that isomerization is limited to a given OH bond orientation. This raises the important question of the scale upon which we can consider ASW to be an amorphous solid. The results of single frequency irradiations suggest that there is a relatively high degree of order, at least at the surface of the ice, which limits the effects of selective irradiation to narrow oscillator classes. The main observed relaxation channel for the energy introduced into the ice by irradiation is the isomerization of a surface mode to the nitrogen-stabilized  $\text{H}_2\text{O}$  monomer. The second interesting point is that we observe no isomerization between the different surface modes upon irradiation. There are thus no secondary relaxation channels via isomerization from one mode to another. We do not discount, but rather advocate for, a large contribution from concerted relaxations via the H-bond network of the bulk of the water ice. However, such a relaxation cannot be observed under our experimental conditions, and thus we can only conclude that surface relaxation is limited to the formation of a new adsorbed  $\text{H}_2\text{O}$  monomer.

What is the mechanism of the isomerization, or reorientation, observed upon selective irradiation and is it the same for all surface modes? If we assume an average water ice H-bond strength<sup>45</sup> of  $\sim 1200 \text{ cm}^{-1}$ , an irradiation in the range 3720–3549  $\text{cm}^{-1}$  could break up to three H-bonds. The  $\text{H}_2\text{O}$  monomer is bicoordinated, while the most tightly bound surface mode, s4, is tetra-coordinated and thus any of the four surface modes could be converted into the monomer by breaking one or two H-bonds. Another possibility that must be considered is that the  $\text{H}_2\text{O}$  molecule desorbs from the surface upon irradiation (as seen in studies of the irradiation of bulk polycrystalline ice<sup>38</sup>) and, in our experiments, readsorbs from the vacuum chamber concurrently with  $\text{N}_2$ . We discount this scenario based upon the following arguments: the area under

the  $3725\text{ cm}^{-1}$  band is of the same order of magnitude for all irradiations, including the s4 mode which can not be directly desorbed with only  $3503\text{ cm}^{-1}$  of energy; there is no evident pressure increase in the vacuum chamber during irradiation, either measured by pressure gauges or upon measuring the masses 18 and 17 ( $\text{H}_2\text{O}$ ) with the mass spectrometer; if low-level desorption does occur, the mean free path of the  $\text{H}_2\text{O}$  molecules is over 1 km, therefore, we would expect no readsorption; and finally, all IR adsorption studies to date have concluded that an adsorbate on a dH provokes a red-shift in the band frequency,<sup>36,46</sup> while the new band is blue-shifted compared to the dH modes in ASW.

Upon comparison of the results of selective irradiation (Figure 3) with those from the annealing experiments (Figure 2), it is clear that the two different methods of introducing energy into the ice, locally in the case of irradiation, and globally upon heating, provoke entirely different modifications of ASW. Where does this difference originate? When the ice is selectively irradiated, we postulate that the majority of the injected energy is relaxed through the H-bonding network of the bulk ice, while only a small part is stored at the surface and in the immediate sublayers. Thus, the vibrational relaxation leading to the formation of a new monomer species is restricted to these few surface layers. A global heating of the ice, however, provokes a rearrangement of the whole ice structure. It is interesting to note that an annealing at 30 K represents a weak input of energy into the whole system (equivalent to  $\sim 21\text{ cm}^{-1}$ ), whereas the irradiations inject between  $3720$  and  $3503\text{ cm}^{-1}$  directly into the surface; the former allows nitrogen to migrate on the ice surface, while the latter allows the partial rearrangement of the  $\text{H}_2\text{O}$  molecules in the ice surface. However, it is clear that the method of energy injection is critical, as the heating distributes energy throughout the whole ASW sample, while the IR photons are selectively delivered by laser to the resonant surface water molecules (including those in pores). A global heating populates phonons, leading to a global rearrangement of the ice while remaining too low in energy to overcome the barrier to the isomerization of dangling molecules. In the case of a selective IR irradiation, the energy, about 180 times larger than that of annealing to 30 K, is directly injected into surface oscillators, after which coupling occurs between oscillators, i.e., intra- and intermolecular vibrational relaxation begins. There is competition between reactional pathways leading to reorientation and those returning to the original potential. Phonons are involved in all of these processes. Considering both the energetics of irradiation and experimental constraints, we conclude that single postdeposition selective irradiations of the surface modes of ASW provoke the reorientation of  $\text{H}_2\text{O}$  molecules at the surface and the formation of a new nitrogen-stabilized  $\text{H}_2\text{O}$  monomer on the ice surface.

**III.C. Multiple Irradiation Experiments.** To further investigate the relaxation of ASW, we performed an experiment where one ASW sample was selectively irradiated consecutively at each of its four surface modes (from red to blue,  $3503\text{ cm}^{-1}$  to  $3720\text{ cm}^{-1}$ ), with each irradiation performed for 1 h (as for the single irradiation experiments presented above). The results of the multiple irradiation experiment are presented in Figure 4. The difference spectra of a single ASW sample consecutively irradiated at  $3503$  (s4, 1),  $3549$  (dO, 2),  $3698$  (dH, 3), and  $3720\text{ cm}^{-1}$  (dH, 4) are presented in the main panel. By comparison with Figure 3, it is clear that the results are very similar to the single irradiation experiments. In fact, the first

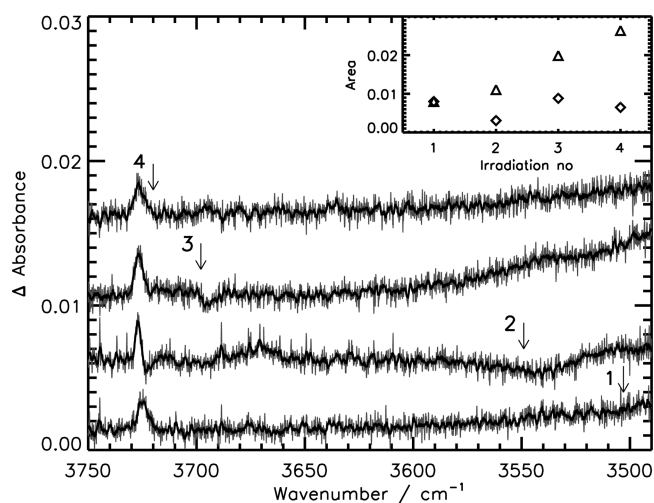


**Figure 4.** Progressive irradiations of an ASW sample from red to blue wavenumbers. Main panel: Spectra in gray are difference spectra taken after irradiation at (1)  $3503\text{ cm}^{-1}$ , (2)  $3549\text{ cm}^{-1}$ , (3)  $3698\text{ cm}^{-1}$ , and (4)  $3720\text{ cm}^{-1}$ . Inset: The area under the band at  $3725\text{ cm}^{-1}$  is plotted for each difference spectrum ( $\diamond$ ) and the cumulative total ( $\triangle$ ).

irradiation (at  $3503\text{ cm}^{-1}$ ) is the same experiment as that presented in section III.B. Upon each irradiation, the band at  $3725\text{ cm}^{-1}$ , attributed to the  $\text{H}_2\text{O}$  monomer, grows. Again, the area under the newly formed band at  $3725\text{ cm}^{-1}$  (corrected for the low level background deposition) is plotted in an inset. In this case, because these irradiations were performed consecutively upon one ASW sample, we also present the cumulative area under the  $3725\text{ cm}^{-1}$  band (plotted as  $\triangle$ ). It is clear that each irradiation provokes the production of a variable number of  $\text{H}_2\text{O}$  monomers and that the cumulative production is not linear with irradiation time. The major difference between the multiple and single irradiations is that for this multiple irradiation experiment we see interconversion between the different surface modes. Irradiation at  $3549\text{ cm}^{-1}$  provokes a “hole-burning” centered at approximately  $3540\text{ cm}^{-1}$  (spectrum 2); after the subsequent irradiation at  $3698\text{ cm}^{-1}$ , there is some repopulation of the dO mode, evidenced by the increase of a wide band at  $\sim 3540\text{ cm}^{-1}$  (spectrum 3). The evidence of interconversion between the surface modes strengthens the hypothesis that some fraction of the energy of irradiation is trapped in the first few layers, causing the isomerization of surface molecules. As the tricoordinated dO is a more stable configuration than the  $\text{H}_2\text{O}$  monomer ( $\Delta\nu \sim 176\text{ cm}^{-1}$ ), it would be a favorable rearrangement for the bicoordinated dH molecules irradiated at  $3698\text{ cm}^{-1}$ . It is possible that in Figure 4, spectra 3 and 4, there is similar evidence of repopulation of the previously depopulated surface mode, but due to noise in the spectra it is not possible to confirm this. The small contribution centered at  $3672\text{ cm}^{-1}$  in spectrum 2 is likely due to the presence of nitrogen. The major product of each of the consecutive irradiations (red to blue) was the  $\text{H}_2\text{O}$  monomer at  $3725\text{ cm}^{-1}$ .

Multiple irradiation experiments from blue to red did not produce the same results as those from red to blue. The results of such a series of experiments is illustrated in Figure 5, where the difference spectra of a single ASW sample consecutively irradiated at  $3720$  (dH, 1),  $3698$  (dH, 2),  $3549$  (dO, 3), and  $3503\text{ cm}^{-1}$  (s4, 4) are presented. Irradiation at  $3720\text{ cm}^{-1}$  (spectrum 1) provokes the formation of a new band at  $3725\text{ cm}^{-1}$  (as well as a weak band at  $3638\text{ cm}^{-1}$ ) as expected for a

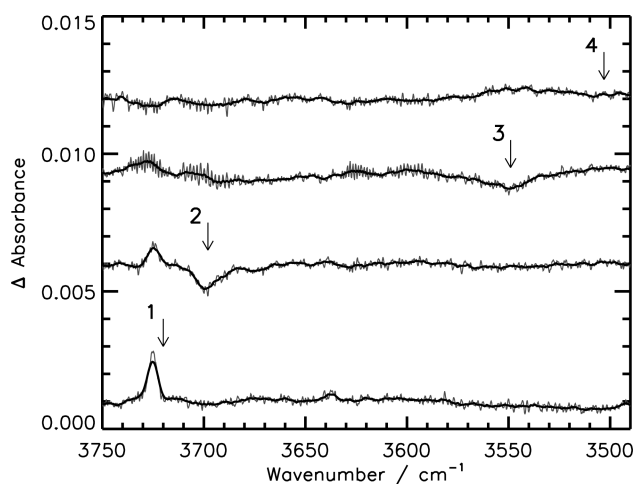


**Figure 5.** Progressive irradiations of an ASW sample from blue to red wavenumbers. Spectra in gray are difference spectra taken after irradiation at (1) 3720  $\text{cm}^{-1}$ , (2) 3698  $\text{cm}^{-1}$ , (3) 3549  $\text{cm}^{-1}$ , and (4) 3503  $\text{cm}^{-1}$ . It is important to note that these spectra were measured using a new model of the same detector used for all other spectra presented in this work (Bruker MCT detector, 4000–800  $\text{cm}^{-1}$ , 0.5  $\text{cm}^{-1}$  resolution, 1000 scans). These spectra have been corrected for changes in the bulk water ice signal.

single irradiation. Subsequent irradiation at 3698  $\text{cm}^{-1}$  (spectrum 2) provokes a decrease in the band at 3699  $\text{cm}^{-1}$  and a continued increase at 3725  $\text{cm}^{-1}$ . The irradiation at 3549  $\text{cm}^{-1}$  provokes a “hole-burning” centered at approximately the irradiation frequency, accompanied by an increase at 3702  $\text{cm}^{-1}$  (suggesting a repopulation of the dH mode) and a weak, broad increase at 3725  $\text{cm}^{-1}$ . This is unlike the behavior of an ice irradiated from red to blue, as in those irradiations, the band at 3725  $\text{cm}^{-1}$  increased by an approximately similar area upon each progressive irradiation. The irradiation at 3503  $\text{cm}^{-1}$  provokes almost no change in the dangling modes of the ice sample. We attribute the decreasing response to irradiation to the fact that we irradiate at the highest energy first, thus introducing more energy into the initial ice sample and provoking more reorganization in the first irradiation. If the least constrained dangling modes, i.e., the dH modes at 3720 and 3698  $\text{cm}^{-1}$  have already been reorganized by irradiation, it is reasonable to assume that subsequent irradiation of more tightly bound molecules, i.e., the dO and s4 modes, will provoke less reorganization.

**III.D. Back Irradiation Experiments.** The third type of irradiation experiment that we performed were irradiations of the 3725  $\text{cm}^{-1}$  band after it had been formed by irradiation of one of the four surface modes. We present the results for two such experiments (initial irradiations at 3720 and 3549  $\text{cm}^{-1}$ ) in Figure 6. The first experiment (Figure 6, spectra 1a,b) presents the results of an irradiation at 3720  $\text{cm}^{-1}$  (spectrum 1a) followed by irradiation at 3725  $\text{cm}^{-1}$  (spectrum 1b). In both difference spectra, the only visible difference is the growth of a band at 3725  $\text{cm}^{-1}$ . The second experiment (Figure 6, spectra 2a,b) is identical, except that the original irradiation frequency is 3549  $\text{cm}^{-1}$ . In this case, we also observe the growth of the 3725  $\text{cm}^{-1}$  band upon both irradiations but also the production of the second  $\text{H}_2\text{O}-\text{N}_2$  complex band at 3638  $\text{cm}^{-1}$ .

Previous selective irradiation studies have shown that, upon irradiation of a newly formed species (particularly one at higher energy than the original molecule), a back conversion from product to original species is possible.<sup>47</sup> However, these studies

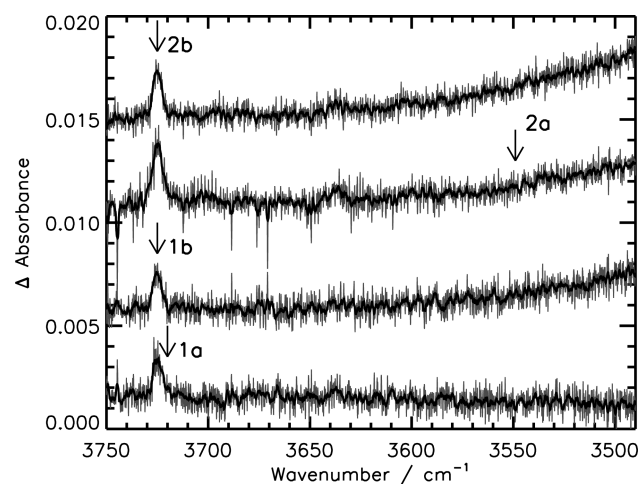


**Figure 6.** Back irradiation of the newly formed 3725  $\text{cm}^{-1}$  band. Spectra in gray are difference spectra taken after irradiation at (1a) 3720  $\text{cm}^{-1}$ , (1b) subsequent irradiation at 3725  $\text{cm}^{-1}$ , (2a) 3549  $\text{cm}^{-1}$ , and (2b) subsequent irradiation at 3725  $\text{cm}^{-1}$ .

were performed in matrixes, and thus the irradiated molecules were isolated in a cage of matrix gas and were not influenced by other molecules of the same species. In this case, we see no back-conversion but rather the newly formed band further increases. The most likely explanation for the continued growth of the band at 3725  $\text{cm}^{-1}$  upon irradiation at 3725  $\text{cm}^{-1}$  is that the wing of the bicoordinated dH band (centered at 3720  $\text{cm}^{-1}$ ) is being irradiated; it is clearly evident in the spectra presented in Figure 1 that a large number of dH oscillators are available for irradiation at that frequency. It is unsurprising that we see no return to the original ASW surface, as the energy injected into the system upon irradiation is approximately enough to break up to three H-bonds. On the basis of this fact, it seems unlikely that the irradiation at 3725  $\text{cm}^{-1}$  will be enough to provoke a back isomerization, which would require a rearrangement of the H-bond network in the surface layers of the ice in order to reinsert the water molecule into the surface. Once again, we see no explicit evidence of desorption of irradiated molecules, despite the relative ease by which a  $\text{H}_2\text{O}$  monomer could be ejected from the surface. We thus deduce that the major vibrational relaxation mode for the injected energy is once again dispersion through the bulk of the ice, despite this being less favorable than it was for molecules in the surface layer of the ice.

#### IV. CONCLUSION AND PERSPECTIVES

In this work we report completely new insights into the IR selective irradiation of ASW dangling modes. It appears that, upon IR irradiation, these molecules are able to isomerize, forming a water monomer which interacts with the ASW surface through its two electronic doublets, while its two OH bonds are complexed by nitrogen molecules. Nitrogen, which is generally considered as a pollutant, reveals the presence of this new mode due to its enhancing effect upon OH dangling modes.

During individual irradiations of the dangling modes we see no interconversion, but this does not necessarily imply that the mechanism for each reorganization is the same and independent of the dangling mode irradiated. Since the energy injected into the system ranges from 3720 to 3503  $\text{cm}^{-1}$ , allowing up to three H-bonds to be broken, the way that this



vibrational energy is relaxed from a bicoordinated dH molecule must not be the same as for a tetra-coordinated s4 molecule. We have established, however, that the isomerized molecules are not ejected from the surface, only to readsorb. The last step of the isomerization process must be a flip to the monomer position after the H-bonds have been broken. The irradiation effects should not be confused with thermal effects, i.e., a global heating of the ice. Heating of ASW provokes an “in phase” global decrease of all of the dangling bonds, whereas upon IR selective irradiation, we observe an “out of phase” decrease in the irradiated dangling bond and the growth of the newly identified  $3725\text{ cm}^{-1}$  band. Because of the narrow “hole burning” events, we can conclude that, although ASW is an amorphous material, only certain classes of oscillator are able to isomerize upon selective irradiation. This then provokes the question: on what scale are these ices truly amorphous? Although we were able to provoke an isomerization of surface water molecules, we were unable to provoke the back-isomerization. This is unsurprising, as a lot more energy would be required to “re-introduce” an  $\text{H}_2\text{O}$  into the H-bonded water network. Indeed, to reintroduce the oscillators at  $3725\text{ cm}^{-1}$  into the H-bonded network, it would be necessary to first break two  $\text{H}_2\text{O}-\text{N}_2$  bonds and two  $\text{H}_2\text{O}-\text{ASW}$  interactions, and then reintroduce at least one of the OH bonds into the surface network. This seems to be a highly unlikely energy relaxation pathway.

The reorganization of the surface upon irradiation clearly alters the catalytic properties of the ASW surface but does not necessarily reduce the catalytic potential. We postulate that, despite the loss of surface dangling modes, the formation of a new bicoordinated  $\text{H}_2\text{O}$  molecule class with two free OH may provide additional surface sites for the adsorption of small molecules. Unlike a global annealing, where there is a clear loss of surface molecules, selective irradiation simply provokes a reorganization of the existing surface. The new arrangement of surface molecules will exhibit its own physical and chemical reactivity. Future studies into the adsorption and catalytic capacities of the reorganized surface are planned. Additionally, we intend to investigate the behavior, upon selective irradiation, of ices polluted by small molecules such as CO or  $\text{CH}_4$ , which are better models of the mixed ices present in the ISM.

## AUTHOR INFORMATION

### Corresponding Author

\*E-mail: stephane.coussan@univ-amu.fr.

### Notes

The authors declare no competing financial interest.

## ACKNOWLEDGMENTS

J. A. Noble is a Royal Commission for the Exhibition of 1851 Research Fellow.

## REFERENCES

- (1) Whittet, D. C. B.; Bode, M. F.; Longmore, A. J.; Baines, D. W. T.; Evans, A. Interstellar Ice Grains in the Taurus Molecular Clouds. *Nature* **1983**, *303*, 218–221.
- (2) Boulter, J. E.; Morgan, C. G.; Marschall, J. Ice Surfaces in the Mesosphere: Absence of Dangling Bonds in the Presence of Atomic Oxygen. *Geo. Res. Lett.* **2005**, *32*, L14817 1–4.
- (3) Leger, A.; Klein, J.; Cheveigne, S. D.; Guinet, C.; Defourneau, D.; Belin, M. The 3.1 Micron Absorption in Molecular Clouds is Probably Due to Amorphous  $\text{H}_2\text{O}$  Ice. *Astron. Astrophys.* **1979**, *79*, 256–259.
- (4) Murray, B. J.; Jensen, E. J. Homogeneous Nucleation of Amorphous Solid Water Particles in the Upper Mesosphere. *J. Atmos. Sol. Terr. Phys.* **2010**, *72*, 51–61.
- (5) Hobbs, P. V. *Ice Physics*; Oxford University Press: London, U.K., 1974.
- (6) Petrenko, V. F.; Whitworth, R. W. *Physics of Ice*; Oxford University Press: New York, 1999.
- (7) Bartels-Rausch, Th.; Bergeron, V.; Cartwright, J. H. E.; Escribano, R.; Finney, J. L.; Grothe, H.; Gutiérrez, P. J.; Haapala, J.; Kuhs, W. F.; Pettersson, J. B. C.; et al. Ice Structures, Patterns, and Processes: A View Across the Icefields. *Rev. Mod. Phys.* **2012**, *84*, 885–944.
- (8) Hama, T.; Watanabe, N. Surface Processes on Interstellar Amorphous Solid Water: Adsorption, Diffusion, Tunneling Reactions, and Nuclear-Spin Conversion. *Chem. Rev.* **2013**, *113*, 8783–8839.
- (9) Debenedetti, P. G. *Metastable Liquids: Concepts and Principles*; Princeton University Press: Princeton, NJ, 1996.
- (10) Tanaka, M.; Sato, S.; Nagata, T.; Yamamoto, T. Three Micron Ice-band Features in the Rho Ophiuchi Sources. *Astrophys. J.* **1990**, *352*, 724–730.
- (11) Knez, C.; Boogert, A. C. A.; Pontoppidan, K. M.; Kessler-Silacci, J.; van Dishoeck, E. F.; Evans, N. J., II; Augereau, J.-C.; Blake, G. A.; Lahuis, F. Spitzer Mid-Infrared Spectroscopy of Ices toward Extincted Background Stars. *Astrophys. J. Lett.* **2005**, *635*, L145–L148.
- (12) Boogert, A. C. A.; Huard, T. L.; Cook, A. M.; Chiar, J. E.; Knez, C.; Decin, L.; Blake, G. A.; Tielens, A. G. G. M.; van Dishoeck, E. F. Ice and Dust in the Quiescent Medium of Isolated Dense Cores. *Astrophys. J.* **2011**, *729*, 92 1–16.
- (13) Noble, J. A.; Fraser, H. J.; Aikawa, Y.; Pontoppidan, K. M.; Sakon, I. A Survey of  $\text{H}_2\text{O}$ ,  $\text{CO}_2$ , and CO Ice Features toward Background Stars and Low-mass Young Stellar Objects Using AKARI. *Astrophys. J.* **2013**, *775*, 85 1–24.
- (14) Greenberg, J. M. Making a Comet Nucleus. *Astron. Astrophys.* **1998**, *330*, 375–380.
- (15) van Dishoeck, E. F. Astrochemistry of Dense Protostellar and Protoplanetary Environments. In *Astrophysics in the Next Decade*; Astrophysics and Space Science Proceedings; Springer Science +Business Media B.V.: Amsterdam, The Netherlands 2009; pp 187–213.
- (16) Hollenbach, D. J.; Salpeter, E. E. Surface Recombination of Hydrogen Molecules. *Astrophys. J.* **1971**, *163*, 155–164.
- (17) Manicò, G.; Ragunì, G.; Pirronello, V.; Roser, J. E.; Vidali, G. Laboratory Measurements of Molecular Hydrogen Formation on Amorphous Water Ice. *Astrophys. J. Lett.* **2001**, *548*, L253–L256.
- (18) Minissale, M.; Congiu, E.; Baouche, S.; Chaabouni, H.; Moudens, A.; Dulieu, F.; Accolla, M.; Cazaux, S.; Manicò, G.; Pirronello, V. Quantum Tunneling of Oxygen Atoms on Very Cold Surfaces. *Phys. Rev. Lett.* **2013**, *111*, 053201 1–5.
- (19) Tielens, A. G. G. M.; Hagen, W. Model Calculations of the Molecular Composition of Interstellar Grain Mantles. *Astron. Astrophys.* **1982**, *114*, 245–260.
- (20) Oba, Y.; Watanabe, N.; Kouchi, A.; Hama, T.; Pirronello, V. Experimental Study of  $\text{CO}_2$  Formation by Surface Reactions of Non-energetic OH Radicals with CO Molecules. *Astrophys. J. Lett.* **2010**, *712*, L174–L178.
- (21) Noble, J. A.; Dulieu, F.; Congiu, E.; Fraser, H. J.  $\text{CO}_2$  Formation in Quiescent Clouds: An Experimental Study of the  $\text{CO} + \text{OH}$  Pathway. *Astrophys. J.* **2011**, *735*, 121 1–6.
- (22) Ioppolo, S.; van Boheemen, Y.; Cuppen, H. M.; van Dishoeck, E. F.; Linnartz, H. Surface Formation of  $\text{CO}_2$  Ice at Low Temperatures. *Mon. Not. R. Astron. Soc.* **2011**, *413*, 2281–2287.
- (23) Tafalla, M.; Myers, P. C.; Caselli, P.; Walmsley, C. M.; Comito, C. Systematic Molecular Differentiation in Starless Cores. *Astrophys. J.* **2002**, *569*, 815–835.
- (24) Parent, P.; Laffon, C. Adsorption of HCl on the Water Ice Surface Studied by X-Ray Adsorption Spectroscopy. *J. Phys. Chem. B* **2005**, *109*, 1547–1553.
- (25) Guennoun, Z.; Couturier-Tamburelli, I.; Pietri, N.; Aycard, J. P. Interstellar Ice Surface Site Modification Induced by Dicyanoacetylene Adsorption. *J. Phys. Chem. B* **2005**, *109*, 3437–3441.

- (26) Watanabe, N.; Kouchi, A. Efficient Formation of Formaldehyde and Methanol by the Addition of Hydrogen Atoms to CO in H<sub>2</sub>O-CO Ice at 10 K. *Astrophys. J. Lett.* **2002**, *571*, L173–L176.
- (27) Danger, G.; Duvernay, F.; Theulé, P.; Borget, F.; Chiavassa, T. Hydroxyacetonitrile (HOCH<sub>2</sub>CN) Formation in Astrophysical Conditions. Competition with the Aminomethanol, a Glycine Precursor. *Astrophys. J.* **2012**, *756*, 11–20.
- (28) Devlin, J. P.; Buch, V. Surface of Ice as Viewed from Combined Spectroscopic and Computer Modeling Studies. *J. Phys. Chem.* **1995**, *99*, 16534–16548.
- (29) Medcraft, C.; McNaughton, D.; Appadoo, D. R. T.; Bauerecker, S.; Robertson, E. G. Water Ice Nanoparticles: Size and Temperature Effects on the Mid-Infrared Spectrum. *Phys. Chem. Chem. Phys.* **2013**, *15*, 3630–3639.
- (30) Collings, M. P.; Anderson, M. A.; Chen, R.; Dewar, J. W.; Viti, S.; Williams, D. A.; Mc Coustra, M. R. S. Laboratory Survey of the Thermal Desorption of Astrophysically Relevant Molecules. *Mon. Not. R. Astron. Soc.* **2004**, *354*, 1133–1140.
- (31) Mennella, V.; Baratta, G. A.; Palumbo, M. E.; Bergin, E. A. Synthesis of CO and CO<sub>2</sub> Molecules by UV Irradiation of Water Ice-covered Hydrogenated Carbon Grains. *Astrophys. J.* **2006**, *643*, 923–931.
- (32) Burton, E. F.; Oliver, W. F. The Crystal Structure of Ice at Low Temperatures. *Proc. R. Soc. A* **1935**, *153*, 166–172.
- (33) Rowland, B.; Devlin, J. P. Spectra of Dangling OH Groups at Ice Cluster Surfaces and Within Pores of Amorphous Ice. *J. Chem. Phys.* **1991**, *94*, 812–813.
- (34) Buch, V.; Devlin, J. P. Spectra of Dangling OH Bonds in Amorphous Ice: Assignment to 2 and 3 Coordinated Surface Molecules. *J. Chem. Phys.* **1991**, *94*, 4091–4092.
- (35) Devlin, J. P.; Buch, V. Vibrational Spectroscopy and Modeling of the Surface and Substructure of Ice and of Ice-Adsorbate Interactions. *J. Phys. Chem. B* **1997**, *101*, 6095–6098.
- (36) Manca, C.; Martin, C.; Roubin, P. Comparative Study of Gas Adsorption on Amorphous Ice: Thermodynamic and Spectroscopic Features of the Adlayer and the Surface. *J. Phys. Chem. B* **2003**, *107*, 8929–8934.
- (37) Noble, J. A.; Martin, C.; Fraser, H. J.; Roubin, P.; Coussan, S. Unveiling the Surface Structure of Amorphous Solid Water via Selective Infrared Irradiation of OH Stretching Modes. *J. Phys. Chem. Lett.* **2014**, *5*, 826–829.
- (38) Focsa, C.; Chazallon, B.; Destombes, J. L. Resonant Desorption of Ice with a Tunable LiNbO<sub>3</sub> Optical Parametric Oscillator. *Surf. Sci.* **2003**, *528*, 189–195.
- (39) Rowland, B.; Fisher, M.; Devlin, J. P. Probing Icy Surfaces with the Dangling OH Mode Absorption: Large Ice Clusters and Microporous Amorphous Ice. *J. Chem. Phys.* **1991**, *95*, 1378–1384.
- (40) Mayer, E.; Pletzer, R. Astrophysical Implications of Amorphous Ice - A Microporous Solid. *Nature* **1986**, *319*, 298–391.
- (41) Hujo, W.; Gaus, M.; Schultze, M.; Kubar, T.; Grunenberg, J.; Elstner, M.; Bauerecker, S. Effect of Nitrogen Adsorption on the Mid-Infrared Spectrum of Water Clusters. *J. Phys. Chem. A* **2011**, *115*, 6218–6225.
- (42) Rudakova, A. V.; Poretskiy, M. S.; Marinov, I. L.; Tsyganenko, A. A. IR Spectroscopic Study of Surface Properties of Amorphous Water Ice. *Opt. Spectrosc.* **2010**, *109*, 708–718.
- (43) Manca, C.; Martin, C.; Roubin, P. Spectroscopic and Volumetric Characterization of a Non-Microporous Amorphous Ice. *Chem. Phys. Lett.* **2002**, *364*, 220–224.
- (44) Coussan, S.; Roubin, P.; Perchard, J. P. Infrared Induced Isomerizations of Water Polymers Trapped in Nitrogen Matrix. *Chem. Phys.* **2006**, *324*, 527–540.
- (45) Nissan, A. H. The Hydrogen-Bond Strength of Ice. *Nature* **1956**, *178*, 1411–1412.
- (46) Manca, C.; Roubin, P.; Martin, C. Volumetric and Infrared Co-Measurements of CH<sub>4</sub> and CO Isotherms on Microporous Ice. *Chem. Phys. Lett.* **2000**, *330*, 21–26.
- (47) Trivella, A.; Wassermann, T. N.; Mestdagh, J. M.; Tanner, C. M.; Marinelli, F.; Roubin, P.; Coussan, S. New Insights Into the Photodynamics of Acetylacetone: Isomerization and Fragmentation in Low-temperature Matrixes. *Phys. Chem. Chem. Phys.* **2010**, *12*, 8300–8310.